Storm disturbances in a Swedish forest-A case study comparing monitoring and modelling

Yu, Lin; Belyazid, Salim; Akselsson, Cecilia; van der Heijden, Gregory; Zanchi, Giuliana

Storm Disturbances in a Swedish Forest—a case study Comparing Monitoring and Modelling

Lin Yu[a,*], Salim Belyazid[a], Cecilia Akselsson[b], Gregory van der Heijden[c] and Giuliana Zanchi[b]

[a] Centre for Environmental and Climate Research, Lund University, Sölvegatan 37, SE-223 62 Lund, Sweden

[b] Department of Physical Geography and Ecosystem Science, Lund University, Sölvegatan 12, SE-223 62 Lund, Sweden

[c] INRA – UR 1138 Biogéochimie des Ecosystèmes Forestiers, route d'amance, 54280 Champenoux, France

Abstract

A Norway spruce (*Picea abies* Karst) forest site in southwest Sweden was chosen to study the effects of storm disturbances over the period 1997–2009, during which two storms, 'Lothar' (Dec. 1999) and 'Gudrun' (Jan. 2005), affected the area. Monitored deposition data, soil water chemistry data and forest inventory data were compared with the predictions of an integrated ecosystem model, ForSAFE, in an effort to reveal and understand the effects of storms on acidification/recovery in forest soils. Both storms caused windthrow loss leading to increased nitrate and sulphate concentrations in soil water as a result of stimulated mineralization. *Lothar* led to increased concentrations of Na^+, Mg^{2+}, and Cl^- in soil water due to sea-salt episode. No general sea-salt episode was seen following *Gudrun*, but small sea-salt episodes were observed in 2007 and 2008. Each sea-salt episode caused a temporary decrease of pH, and a subsequent recovery, but overall, the soil water pH decreased from 4.54 to 3.86 after *Lothar*. Modelling suggested that the site was recovering from acidification from 1990s, and would continue to recover in future. Both modelled and monitored data showed that storm caused disturbances in the recovery; monitored data even suggested that soil acidification happened due to storm disturbances. Sea-salt episode does not increase soil acidity in the long term, and will probably decrease the soil acidity by replenishing the base saturation. The modelled data also suggested that storms with only windthrow would not have effects on soil acidification recovery in the long term, but they may influence the soil fertility by losses of base cations.

---

* Corresponding author. Tel.: +46 46 222 86 34.
E-mail addresses: lin.yu@cec.lu.se (L. Yu), salim@belyazid.com (S. Belyazid), cecilia.akselsson@nateko.lu.se (C. Akselsson), gregory.vanderheijden@nancy.inra.fr (G. van der Heijden), giuliana.zanchi@nateko.lu.se (G. Zanchi).

29

1. Introduction

Swedish forests generally grow on nutrient-poor soils, mainly tills from nutrient-poor bedrocks such as granites and gneisses (Wastenson et al. 1990). The fertility of these soils has been further affected by acid deposition (Reuss & Johnson 1986). Furthermore, whole-tree harvesting has become more common in recent decades, leading to further removal of base cations (Iwald et al. 2013; Akselsson et al. 2007; Brandtberg & Olsson 2012). One main effect of acid deposition (S and N) on forest soils is the increased leaching of sulphate and nitrate coupled with nutrient cations such as Mg^{2+}, Ca^{2+} and K^+ causing base cations (BC: Ca^{2+}, Mg^{2+}, K^+) depletion from the soil (Reuss & Johnson 1986). Base cations depletion in forest soils due to high acid deposition has been simulated in several model approaches in regional scale (Sverdrup & Rosen 1998; Akselsson et al. 2007) and in catchment scale (Navrátil et al. 2007; HruŠka et al. 2012; Oulehle et al. 2007). However, the N deposition in most of Sweden is generally low (Simpson et al. 2011), and northern forest ecosystems are normally nitrogen (N) limited (Tamm 1991; Jonard et al. 2015). Thus, leaching of inorganic nitrogen is generally very low in Swedish forests, except for the southwesternmost part with the highest present and historical N deposition, where the nitrate concentration in soil water is often elevated (Akselsson et al. 2010).

S deposition to forest ecosystems has strongly decreased since the 1990s throughout Sweden, but recovery from acidification has been reported to be very slow (Pihl Karlsson et al. 2011; Akselsson et al. 2013). This has also been demonstrated through dynamic modelling (Sverdrup et al. 2005), and can be explained by the slow replacement, through weathering and deposition, of the base cations that were lost during acidification. Although N deposition has decreased in some areas of Sweden, it has generally remained constant (Pihl Karlsson et al. 2011). N accumulation in forest soils due to high loads of N deposition is also preoccupying for soil acidification recovery. In forest soils with high N content, intense N leaching episodes may occur following ecosystem disturbances such as clear-cutting (Gundersen et al. 2006; Zanchi et al. 2014), or windthrow from storms (Legout et al. 2009). Intense N leaching episodes, for which no causal explanation was found, have also been reported (van der Heijden et al. 2011). The consequences of such episodes are increased acidity and increased aluminum concentrations in soil solution, along with increased leaching of base cations and aluminum (e.g. Lundell et al. 2001). In the long term, N leaching although episodic may strongly impact the recovery from soil acidification.

Natural ecosystem disturbances, such as storms, droughts and fire, may also have considerable effects on the physical, chemical and biological properties of the soil, and thus the soil fertility. Storms are one of the most common types of ecosystem disturbances in Swedish forests (Schlyter et al. 2006). Storms are high-wind episodes, sometimes accompanied by heavy rain, which may lead to a reduction in canopy closure due to windthrow and stem breakage, thereby also increasing solar radiation levels in stands (Vodde et al. 2011). Storms may also lead to an increase in the availability of nutrients and water (Vygodskaya et al.

64 2002; Legout et al. 2009), as a result of the reduced uptake and the increase in woody debris which will

65 decompose and release nutrients (Vodde et al. 2011). In fact, the stimulation of mineralization of organic

66 matter, particularly the rate of nitrification, has been reported to be an important change resulting from

67 ecosystem disturbances (Attiwill & Adams 1993; Dahlgren & Driscoll 1994; Legout et al. 2009). This is

68 often accompanied by the leaching of nitrate and BC (Dahlgren & Driscoll 1994).

69 Apart from the effect of wind on trees, storms with high precipitation often cause sea-salt episodes. Sea-

70 salt episodes affect the cation exchange in soil; and is known as the 'sea-salt effect' (Hindar et al. 1995).

71 The cations transported by sea-salt episodes, primarily Na^+ and Mg^{2+}, cause the displacement of absorbed

72 acid ions: hydrogen (H^+), labile aluminum (Al^{3+}) (Wright et al. 1988; Evans et al. 2001), and other BC:

73 Ca^{2+} and K^+ (Hindar et al. 1994; Hindar et al. 1995). The relationship between soil acidity and the leaching

74 of H^+, Al^{3+} and base cations is complex, but it is often observed that the pH falls and Al^{3+} increases and

75 sea salt ions (Na^+, Mg^{2+}, and Cl^-) increase shortly after sea-salt episodes (Hindar et al. 1995; Pedersen &

76 Bille-Hansen 1995). Disturbances in acidification recovery as a result of sea-salt episodes have been

77 observed in European and Swedish forests (Wright 2008; Akselsson et al. 2013; Laudon 2008). Wright

78 observed that sea-salt episodes were responsible for more than one-third of the low ANC (ANC < −50

79 $\mu eq\ l^{-1}$) episodes, which were considered as strong indicator of acid episodes, at Birkenes in Norway

80 during the period 1975–2004. Akselsson et al. (2013) and Laudon (2008) pointed out that recovery from

81 acidification was slow at some coastal forest sites in Sweden, as these sites are susceptible to sea-salt

82 episodes.

83 The aim of this study was to investigate the effects of storms on the acidification/recovery processes in

84 forest soils. We hypothesized that: the high deposition of sea salt and increased rate of nutrient

85 mineralization caused by storms slow down the recovery trend of forest soils from past acidification. For

86 this purpose, a site in southwest Sweden that suffered the effects of the storms 'Lothar' and 'Gudrun' was

87 studied. ForSAFE, a numerical model simulating biogeochemical cycling in forest ecosystems, was

88 applied with monitoring data from the site. Both monitoring data and modelled data were used to study the

89 acidification/recovery trends and the influence of the storms 'Lothar' and 'Gudrun' on these trends.

90 Finally, ForSAFE was used to simulate the influence of frequently occurring storms in the future on soil

91 acidification recovery.

2. Materials & Methods

2.1. Site description

94 The study site, was a 30 × 30 m square plot located in a forest called Klintaskogen (55º 62'N, 13º 44'E) in

95 the region of Scania (southwest Sweden), and is part of the Swedish Throughfall Monitoring Network

96 (SWETHRO) (Pihl Karlsson et al. 2011). It is also one of 223 intensive monitoring plots managed by the

97   Swedish Forest Agency. The average annual precipitation at Klintaskogen is 780mm and the average
98   annual temperature is 7.2 °C (average over 1961–2010). The site is about 25 km from the west coast and
99   about 30 km from the south coast of Sweden. The elevation of Klintaskogen is about 105 m, and it is on
100   the southwestern slope of the horst Romeleåsen.

101   Klintaskogen is a managed Norway spruce (*Picea abies* Karst) forest that was planted on a juniperous
102   grass-land in the 19th century. The latest final felling occurred in 1957, and the site was replanted with
103   Norway spruce. Klintaskogen suffered from the severe wind storm *Lothar* in Dec. 1999, which caused
104   windthrow of about 15% of the trees in the study plot. Another wind storm, *Gudrun,* also caused damage
105   at the study site in January 2005, but tree loss (about 5% of the trees) was less severe.

106   The forest floor has a thin organic layer (3.5 cm) with 48% organic matter content (Loss on Ignition, LOI)
107   (Table 1). The soil type is dystric regosol. The top 50 cm of the mineral soil profile is sandy and acidic
108   with very low base saturation, and the exchange sites are mainly occupied by Al^{3+} (Table 1). The organic
109   matter content decreases downwards from 10.8% to 2.3%, and the pH_{H2O} increases downwards from 4.2 to
110   5.0, within the top 50 cm of soil (Table 1).

111   **2.2. Monitoring data**
112   The following parameters are monitored at the Klintaskogen site:

113   a)   **Deposition:** Thoughfall was collected monthly between 1997 and 2009 with a total of ten
114   throughfall collectors along two sides of the study plot. Bulk rainfall was collected monthly in an
115   open-field collector between 1997 and 2001.
116   b)   **Soil solution chemistry:** Soil solution was collected at 50 cm depth using tension cup lysimeters
117   (5 replicates), three times per year from 1997 to 2009. The 5 sample obtained were combined into
118   a composite sample on each sampling occasion for the analysis of: sulphate (SO_4^{2+}), Cl^-, nitrate
119   (NO_3^-), ammonium (NH_4^+), Ca^{2+}, Mg^{2+}, Na^+, K^+, Mn^{2+}, Fe^{3+}, inorganic Al (iAl), organic Al (oAl)
120   and dissolved organic carbon (DOC). Composite samples with volumes <50 ml were not analyzed.
121   The ANC was computed as follows:
122     $$ANC = [Ca^{2+}] + [Mg^{2+}] + [K^+] + [Na^+] + [NH_4^+] - [SO_4^{2-}] - [Cl^-] - [NO_3^-] \quad (1)$$
123   where the concentrations are in the units eq l^{-1}.
124   c)   **Forest inventories:** Inventories were carried out on three occasions (1996, 1999 and 2004) within
125   the intensive monitoring program led by the Swedish Forest Agency, and these inventories were
126   complemented with an inventory in 2010, using the same methodology. On each occasion, the
127   diameter at breast height of each tree was measured, and the tree and crown heights were
128   measured in a selected aliquot representing 20% of the trees in the plot.

129   d) **Soil characteristics:** In 2010, soil samples were collected and C, N, pH, exchangeable cations,

130   grain size distribution, bulk density and total element contents were determined. Total element

131   analysis was accomplished by ALS Scandinavia AB in Agrilab Uppsala in 2010.

132 The properties of the soil at the study site are given in Table 1, and a detailed description of the

133 SWETHRO network monitoring equipment and analysis protocols has been given in Pihl Karlsson et al.

134 (2011).

135 Table 1

136 Soil properties at Klintaskogen

Horizon	Layer thickness	Stoniness[a]	pH		Exchangeable ions, µeq/g								CEC[b]	BS	Tot-C	Tot-N	Grain size[c]		
	m	Fraction	H_2O	KCl	Fe	Mn	Al	H	Na	K	Mg	Ca	10^{-5} kmolc/kg	%	g/Kg DS	g/Kg DS	Clay	Silt	Sand
O	0.035	0	4.1	3.2	3.5	12.1	27.6	47.9	<0,1	4.6	11.7	71.1	17.9	49.0	312.9	15.0	–	–	–
A	0.06	0.15	4.2	3.3	3.3	0.7	55.4	24.6	<0,1	1.4	1.8	7.5	9.47	11.2	61.5	3.8	4	24	72
AB	0.08	0.15	4.5	3.8	0.8	0.3	41.5	11.0	<0,1	0.7	0.6	1.8	5.67	5.0	32.4	2.2	4	24	72
B	0.16	0.15	4.8	4.2	0.2	0.1	21.1	3.9	<0,1	0.4	0.1	0.9	2.66	5.4	13.8	1.1	8	20	72
C	0.2	0.15	5.0	4.2	0.1	0.1	15.4	3.2	<0,1	0.5	0.4	2.0	2.17	13.4	10.4	0.9	6	18	76

137   [a] The fraction of stones and boulders was assessed visually.

138   [b] CEC: cation exchange capacity; BS: base saturation.

139   [c] Grain size is expressed in percent.

140 **2.3. Calculations**

141 *2.3.1. Tree biomass*

142 The biomass of stems, branches, needles, and fine roots was estimated for each tree using Marklund

143 functions (Marklund 1988). The biomass of each tree compartment (wood, needles, and fine roots) of each

144 tree within the study plot were calculated and summed to provide an estimate of the standing biomass per

145 square meter, where wood referred to the sum of stems and branches.

146 *2.3.2. Atmospheric deposition in study plot*

147 The total atmospheric deposition (TD) was calculated as the sum of wet (bulk precipitation deposition)

148 and dry deposition. For sulphate, nitrate, Na^+ and Cl^-, canopy exchange is assumed to be zero. Dry

149 deposition is thus the difference between throughfall deposition and bulk precipitation deposition. The dry

150 deposition of BC was computed using the Na dry deposition factor (Staelens et al. 2008):

151    $$DD_x = \frac{(TFD-PD)_{Na}}{PD_{Na}} PD_x \qquad (2)$$

152 where DD_x is the dry deposition of element x, TFD is the throughfall deposition, and PD is the open-field

153 precipitation deposition.

154 Annual deposition was computed, except for years in which values of monthly throughfall and/or bulk
155 precipitation data were missing. The total annual deposition of BC and Na^+ was only available for 1998,
156 1999 and 2001; the total annual deposition of ammonium was only available from 1996 to 2001. Missing
157 values were estimated as follows:

158   1) The main source of Mg^{2+} and Na^+ deposition was assumed to be sea salt. Therefore, the average
159   values of $\frac{TD_{Mg}}{TD_{Cl}}$ and $\frac{TD_{Na}}{TD_{Cl}}$ in 1998, 1999 and 2001 were used to estimate missing TD of Mg^{2+} and
160   Na^+ from measured TD of Cl^-.
161   2) Ca^{2+} and K^+ deposition was assumed to be constant over the period. The average TD for the years
162   1998, 1999 and 2001 were used to estimate missing values.
163   3) No PD measurements of BC or Na^+ were available from 2002 to 2009, so it was not possible to
164   calculate the TD of ammonium by canopy exchange model. Therefore, the downscaled data for
165   ammonium from the European Monitoring and Evaluation Programme (EMEP) were used.

166 *2.3.3. Statistical tools*

167 All statistical tests were carried out with the RStudio software (R Core Team 2013). Temporal trends in
168 atmospheric deposition and soil solution concentration were tested with the Mann-Kendall test of the
169 Kendall R package (McLeod 2011). Correlations between major element concentrations in soil solution
170 were tested with the Pearson test. For both tests, $p<0.05$ indicates statistical significance, and $p<0.001$
171 indicates strong statistical significance.

172 **2.4. The ForSAFE model**
173 ForSAFE is a mechanistic model designed to simulate the dynamic responses of forest ecosystems to
174 environmental changes (Figure 1). A full description of the model can be found in the literature (Belyazid
175 et al. 2006; Wallman et al. 2005).

176 Simulations with the ForSAFE model were run over the period 1800 to 2100, and the model was
177 calibrated over the period 1997–2009 using the monitoring data collected from the Klintaskogen site
178 described above. The ForSAFE inputs (soil properties, climate, deposition and silviculture scenario) are
179 described below, and the values used are given in Table 2 and Table 3.
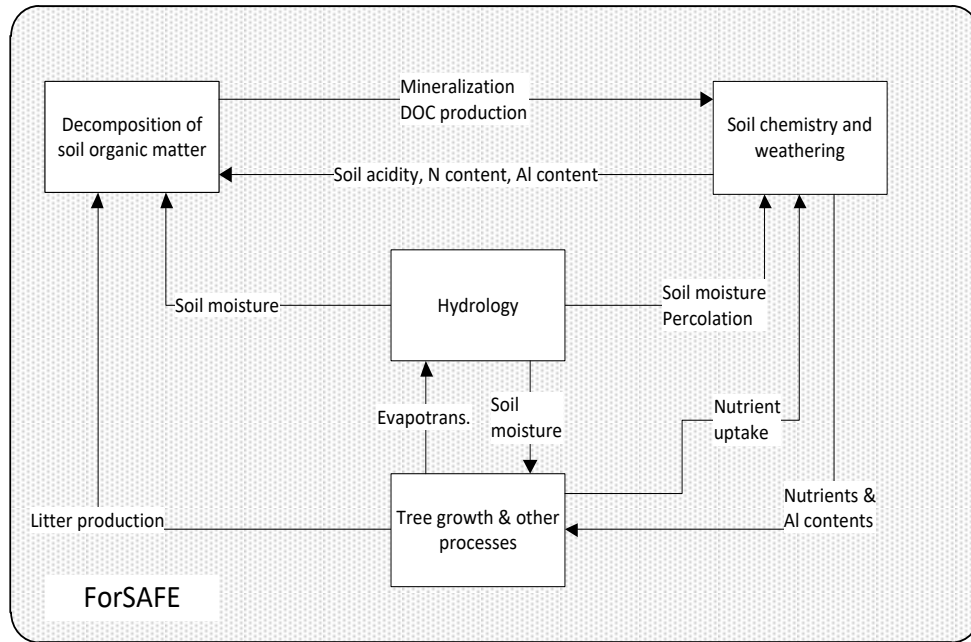
180

Figure 1. Layout of the ForSAFE model, showing the connections/interactions between the four sub-modules: decomposition, soil chemistry, hydrology and tree.

181

182

2.4.1. Soil inputs

The 50 cm soil profile was divided into 5 layers in accordance with the soil measurements (Table 2). Exposed surface areas of minerals were calculated using bulk density and grain size (Warfvinge & Sverdrup 1995; Sverdrup & Warfvinge 1993). The partial pressure of CO_2 (pCO_2) and the aluminium solubility (K_{gibb}) were derived from Warfvinge & Sverdrup (1993) and Sverdrup & Warfvinge (1995). Root fractions were derived for each layer based on the empirical data by Rosengren & Stjernquist (2004). Mineralogical regions from Warfvinge & Sverdrup (1995) were used to assess the potential mineral occurrence in the geographical area. Based on this, and the total element analysis, soil mineral composition was determined using A2M model (Posch & Kurz 2007) (Table 3).

The soil field saturation points for each soil layer were calculated as follows:

$$FS = 1 - \frac{BD \cdot (1-HML) \cdot LOI}{\rho_{organic}} - \frac{BD \times (1-LOI)}{\rho_{particle}} \tag{3}$$

where FS is the field saturation ($m^3_{water}\ m^{-3}_{soil}$), BD is the bulk density (kg m^{-3}), HML is the heat mass loss from 40 °C to 105 °C (fraction of weight), LOI is the loss on ignition (fraction of weight), $\rho_{organic}$ is the density of organic matter, assumed to be 600 kg m^{-3}, and $\rho_{particle}$ is the density of sand particles, assumed to be 2670 kg m^{-3} (Milsom 2003). The field capacity (FC), wilting point (WP) were calculated using the

8

198 method described by Balland et al. (2008). The cation exchange capacity and base saturation were
199 calculated from measured soil properties in Table 1.

200 *2.4.2. Climate inputs*

201 The climate input data included precipitation, maximum, minimum & average temperature, atmospheric
202 CO_2 concentration and radiation for the period 1800–2100. A weather station belonging to the Swedish
203 Meteorological and Hydrological Institute (SMHI) situated about 12km southwest of the Klintaskogen site
204 measured daily precipitation and temperature for the period 1961 to 2010 period. Precipitation and
205 temperature data for the period 2010–2100 were derived from the global climate model HADLEY (Johns
206 et al. 2006) follows the SRESA2 emission story-line of the Intergovernmental Panel on Climate Change
207 (Nakicenovic et al. 2000). For the period 1900–1960, data were estimated by repeating the measured
208 values for 1960–1990 twice. For the period 1800–1900, data were estimated by repeating the measured
209 climate data for the year 1960. The CO_2 concentrations from 1970 to 2100 were derived from the SRESA2
210 scenario. The CO_2 concentration in 1800 was obtained by extrapolation, assuming that it remained
211 constant before 1970. Solar radiation data for 1960–2100 were derived from a study performed by the
212 Regional Climate Group at the University of Gothenburg (David Rayner, personal communication). Solar
213 radiation data were extrapolated back to 1800 using the same scheme for precipitation and temperature
214 data. To avoid the need to calibrate the modeled interception of precipitation, the precipitation data were
215 further scaled to give the throughfall precipitation using the monitored throughfall precipitation factor:

216 $$TFprec_x = \frac{TFprec_{1997-2009}}{Prec_{1997-2009}} Prec_x \qquad (4)$$

217 where $TFprec_x$ is the throughfall precipitation for month x, $Prec_x$ is the precipitation during month x,
218 $TFprec_{1997-2009}$ is the total throughfall precipitation monitored by the SWETHRO network from 1997 to
219 2009, and $Prec_{1997-2009}$ is the total precipitation obtained from the SMHI station from 1997 to 2009.

220 *2.4.3. Deposition inputs*

221 The deposition input data included the atmospheric deposition of sulphate, nitrate, and ammonium, Ca^{2+},
222 Mg^{2+}, K^+, Cl^- and Na^+ in intervals of one year. The Current Legislation (CLE) scenario and the
223 Gothenburg protocol for the UN Convention on Long-Range Transboundary Air Pollution provided by the
224 EMEP on a 50×50 km grid was used to estimate atmospheric deposition data during the period 1800–
225 2100. The EMEP data include deposition of sulphate, nitrate and ammonium from 1900 to 2100. EMEP
226 data were downscaled by the average ratio of the measured deposition to the EMEP deposition (1997–
227 2009) for sulphate, nitrate and ammonium. Atmospheric deposition was assumed to be constant and equal
228 to the deposition in 1900 during the period 1800–1900. The deposition of Ca^{2+}, Mg^{2+}, K^+, Cl^- and Na^+ was
229 assumed to be constant over the simulation period (1800–2100) and equal to the average measured

230 deposition for each element. The yearly deposition input was converted to monthly amounts in ForSAFE

231 assuming that the monthly deposition is proportional to the monthly amount of precipitation.

232 *2.4.4. Storm disturbance and the future storm disturbances scenario*

233 Windthrow caused by the storms was implemented in ForSAFE by simulating thinning at the end of 1999

234 to model the effects of *Lothar*, reducing the standing biomass by 15%, and thinning in 2005 to account for

235 *Gudrun*, reducing the standing biomass by 5%. The stimulation of organic matter mineralization in soils

236 was implemented in the model by reducing the nutrient immobilization in microbial biomass after each

237 storm. It was assumed that the reduction was greatest after storm, and the initial immobilization level was

238 recovered after three years.

239 A scenario involving future storm disturbances (FSS) was included in the study for comparison with the

240 baseline scenario (BLS). In the FSS scenario, it was assumed that a storm would occur every 20 years

241 from 2005 onwards, causing 10% windthrow loss and stimulating organic matter mineralization (as

242 described above) at each storm occurrence. All the storms are assumed not to be accompanied with sea-

243 salt episodes. The difference in soil nutrient input-output budgets between the BLS and the FSS was

244 determined using the model. No silvicultural thinning or harvesting was included in either scenario after

245 the clear-cut in 1957 in order that only effects of storm are identified.

246 **2.5. Nutrient input-output budget calculation**

247 Nitrogen and base cations input-output budgets were calculated over the period 1970–2070 for the two

248 scenarios using the methodology applied in many other studies (Sverdrup et al. 2006; Akselsson et al.

249 2007; van der Heijden et al. 2013). Nutrient budgets were calculated as the difference between soil inputs

250 and outputs. At the forest plot scale, nutrient budgets can be adapted from Ranger & Turpault (1999):

251 $$B(N) = AD(N) + F(N) - U(N) - L(N) \qquad (5)$$

252 $$B(BC) = AD(BC) + W(BC) - U(BC) - L(BC) \qquad (6)$$

253 where B(x) is the nutrient budget of x, AD(x) is total annual atmospheric deposition of x, F(N) is the

254 fixation of N in the soil, assumed to be 0.12 kmolc ha^{-1} y^{-1} (DeLuca et al. 2002), and W(BC) is the

255 weathering of BC. U(x) is the net accumulation of x in wood biomass, and L(x) is the leaching flux of x at

256 50 cm depth. All fluxes and budgets are expressed in kmolc ha^{-1} y^{-1}. The plant uptake of N and BC,

257 leaching of N and BC and weathering of BC were computed with ForSAFE.

258

259 Table 2

260 ForSAFE inputs of soil properties for the plot at Klintaskogen

Layer	$z^{a,b}$ (m)	Density (kg m^{-3})	Area (10^6 m^{-2})	pCO$_2$	K$_{gibb}$	FC (m^{3}water m^{-3}soil)	WP (m^{3}water m^{-3}soil)	LP (m^{3}water m^{-3}soil)	FS (m^{3}water m^{-3}soil)	Roots fraction
1	0.035	195	0	10	6.5	0.410	0.150	0.258	0.687	0.2
2	0.051	709	754052	10	6.5	0.299	0.099	0.212	0.565	0.2
3	0.068	957	1017944	20	7.6	0.338	0.093	0.203	0.542	0.28
4	0.136	1393	1805718	20	8.6	0.332	0.089	0.180	0.481	0.22
5	0.17	1258	1389149	20	9.2	0.306	0.076	0.160	0.428	0.1

261 [a] Data are based on the results of lab analysis of the soil samples listed in Table 1 (see text for detailed explanation).

262 [b] z is the corrected layer depth; Density is bulk density; Area is exposed surface area of minerals; The other abbreviations have been

263 defined in the text.

264 Table 3

265 ForSAFE inputs of soil minerals for the Klintaskogen plot

Layer	Quartz[a]	Plagioclase Albite	Anorthite	Hornblende	Illite	Epidote	Vermiculite1	Vermiculite2	Chlorite1	Chlorite2	Muscovite	Apatite	K-Feldspar	Hematite	Rutile
1	16.59[b]	5.15	1.02	1.01	0.63	0.86	1.17	0.31	0.53	0.34	2.45	0.49	3.44	1.03	0.32
2	55.07	9.34	1.84	1.04	1.72	1.63	1.52	0.59	0.9	0.61	3.3	0.26	6.87	2.34	0.72
3	55.95	10.07	2.12	1.93	1.29	1.79	2.32	0.64	1.09	0.69	4.7	0.24	6.37	2.05	0.73
4	58.11	11.77	3.09	2.67	2.64	1.32	0.5	0.39	2.02	1.7	2.86	0.26	9.42	2.05	0.65
5	50.19	14.25	1.92	1.35	2.09	2.35	4.48	0.74	1.27	0.79	4.11	0.28	10.81	1.03	0.5

266 [a] Quartz: SiO$_2$, Albite: NaAlSi$_3$O$_8$, Anorthite: CaAl$_2$Si$_2$O$_8$, Hornblende: K$_{18}$Na$_{54}$Ca$_{166}$Mg$_{210}$Fe$_{180}$Ti$_{11}$Al$_{216}$Si$_{606}$O$_{2146}$(OH)$_{188}$,

267 Illite: K$_{0.6}$Al$_2$(Al$_{0.6}$Si$_{3.4}$O$_{10}$)(OH)$_2$, Epidote: Ca$_{80}$Fe$_{30}$Al$_{96}$Si$_{124}$O$_{495}$(OH)$_{44}$, Vermiculite1: Ca$_{20}$Mg$_{103}$Fe$_{182}$Al$_{162}$Si$_{293}$O$_{832}$(OH)$_{804}$,

268 Vermiculite2: Ca$_{10}$Mg$_{103}$Fe$_{22}$Al$_{68}$Si$_{123}$O$_{249}$(OH)$_{490}$, Chlorite1: Na$_2$Ca$_3$Mg$_{107}$Fe$_{124}$TiAl$_{124}$Si$_{138}$O$_{540}$(OH)$_{442}$,

269 Chlorite2: Mg$_{103}$Fe$_{58}$TiAl$_{100}$Si$_{87}$O$_{365}$(OH)$_{302}$, Muscovite: K$_{44}$Na$_2$Mg$_8$Fe$_{12}$Ti$_2$Al$_{96}$Si$_{120}$O$_{390}$(OH)$_{94}$, Apatite: Ca$_{10}$(PO$_4$)$_6$(OH)$_2$, K-Feldspar: KAlSi$_3$O$_8$,

270 Hematite: Fe$_2$O$_3$, Rutile: TiO$_2$. (Warfvinge & Sverdrup 1995)

271 [b] the values given are the percent of the total weight in the soil layer. Water content and organic material content are not presented in

272 the table.

273

274

3. Results

3.1. Monitoring data from the study plot

3.1.1. Atmospheric deposition 1997–2009

The total deposition of Cl⁻, sulphate, nitrate and ammonium is shown in Figure 2. Chloride was the most abundant anion in atmospheric deposition, with an average deposition rate of 1.33 kmolc ha⁻¹ y⁻¹. Sulphate was the second most abundant anion with an average deposition rate of 0.35 kmolc ha⁻¹ y⁻¹. The total N deposition was 1.39 kmolc ha⁻¹ y⁻¹ (nitrate: 0.66 kmolc ha⁻¹ y⁻¹; ammonium: 0.73 kmolc ha⁻¹ y⁻¹). Cl⁻ deposition showed a peak in 2000 (3.76 kmolc ha⁻¹ y⁻¹), and a small increase after 2006. Sulphate deposition decreased significantly (τ=–0.684, p=0.001) from about 0.5 kmolc ha⁻¹ y⁻¹ in 1997 to about 0.25 kmolc ha⁻¹ y⁻¹ in 2009. Ammonium deposition also decreased significantly, from 0.88 kmolc ha⁻¹ y⁻¹ to 0.63 kmolc ha⁻¹ y⁻¹, over the same period (τ=–0.615, p=0.004). However, nitrate deposition and total N deposition were relatively stable over the period.
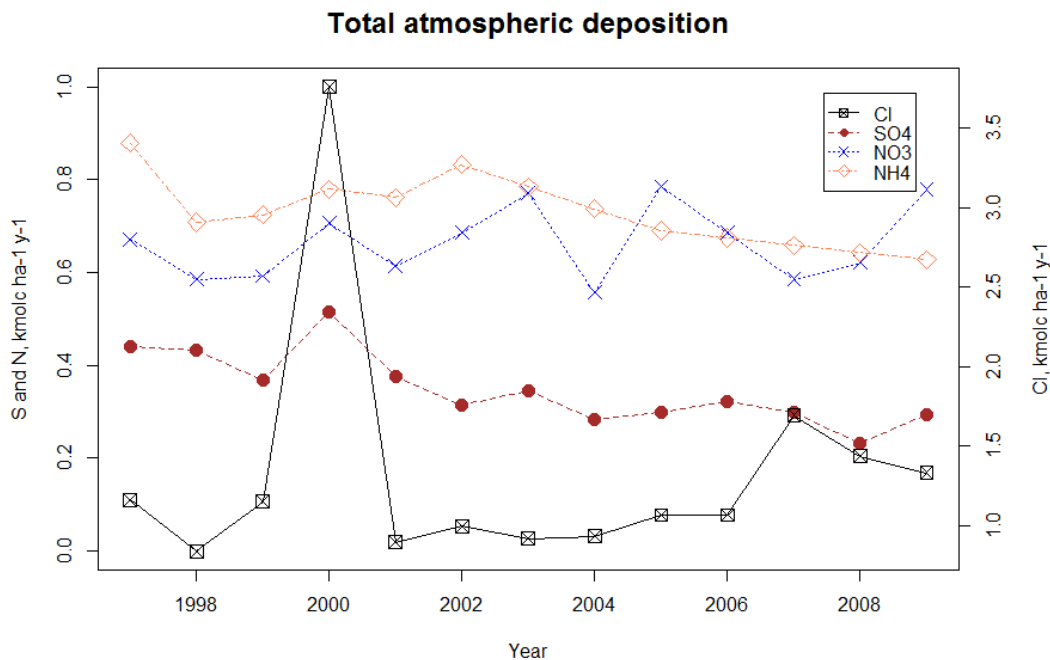
Figure 2. Total atmospheric deposition of Cl⁻, sulphate, nitrate and ammonium over the period 1997–2009 at the study plot in Klintaskogen.

Total atmospheric deposition of Na⁺, Ca²⁺, Mg²⁺ and K⁺ is given in Table 4. The average Na⁺ deposition for the years 1998, 1999 and 2001 was 0.84 kmolc ha⁻¹ y⁻¹, while the average deposition of Ca²⁺, Mg²⁺ and K⁺ over the same period were 0.095, 0.10 and 0.057 kmolc ha⁻¹ y⁻¹, respectively. The monthly deposition (data not shown) of K⁺ showed a decreasing tendency over the period 1998–2001 (τ=–0.306,

293   p=0.007), and the monthly deposition of Ca^{2+} also seemed to decrease however this visual trend was not

294   statistically significant (τ=–0.215, p=0.06). No significant trends were seen in the monthly Na^+ and Mg^{2+}

295   deposition over the same period.

296   Table 4

297   Total atmospheric deposition of Na, Ca, Mg and K (kmolc ha^{-1} y^{-1})

| Year	Na	Ca	Mg	K
1998	0.72	0.092	0.092	0.065
1999	1.07	0.10	0.14	0.067
2001	0.73	0.094	0.080	0.039
Average	0.84	0.095	0.10	0.057

298

299   *3.1.2. Soil solution chemistry 1997–2009*

300   The soil water at the study site over the period 1997–2009 was acidic. The pH ranged from 3.86 to 4.54,

301   and the ANC was negative, ranging from about –600 to about –100 µeq l^{-1}, as can be seen in Figure 3. The

302   dominant anion was Cl^-, and the dominant cation was Na^+. The concentrations of Na^+ and Cl^- increased

303   significantly over the whole period monitored (Cl, τ=0.448, p<0.001; Na, τ=0.458, p<0.001), while Ca^{2+}

304   and ANC decreased (Ca, τ=–0.292, p=0.02; ANC, τ=–0.3, p=0.02). However, the trend analysis before

305   *Lothar* and after *Lothar* gave different results. Before *Lothar*, the nitrate concentration decreased (τ=–

306   0.491, p=0.04). After *Lothar*, the pH and Ca^{2+} concentration decreased significantly (pH, τ=–0.602,

307   p<0.001; Ca, τ=–0.568, p<0.001), while Cl^- and DOC increased significantly (Cl, τ=0.368, p=0.03; DOC,

308   τ=0.459, p=0.02). High concentrations of Cl^-, nitrate, sulphate, Na^+, Ca^{2+}, Mg^{2+} and oAl were noted in

309   2000.

310   Over the period monitored, the Cl^- concentration was significantly positively correlated with the

311   concentrations of Na^+ and Mg^{2+} (Na: R^2=0.746, p<0.001; Mg: R^2=0.606, p<0.001), but not the Ca^{2+} and

312   K^+ concentrations. Interestingly, Cl^- showed the same positive correlations with Na^+ and Mg^{2+} after

313   *Lothar* (Na: R^2=0.615, p=0.004; Mg: R^2=0.522, p=0.02), but it was not correlated with any cations before

314   *Lothar*. The nitrate concentration was positively correlated with Na^+, Mg^{2+} and Ca^{2+} (Na: R^2=0.491,

315   p=0.006; Mg: R^2=0.800, p<0.001; Ca: R^2=0.526, p=0.003) over the period 1997–2009. Both Mg^{2+} and

316   Ca^{2+} showed positive correlations with nitrate before and after *Lothar*, but no other correlations with

317   nitrate were found before or after *Lothar* for the other elements. The pH was significantly negatively

318   correlated with DOC concentration (DOC: R^2=0.651, p<0.001) during the period 1997–2009. The pH was

319   also negatively correlated with DOC both before and after *Lothar*.

320
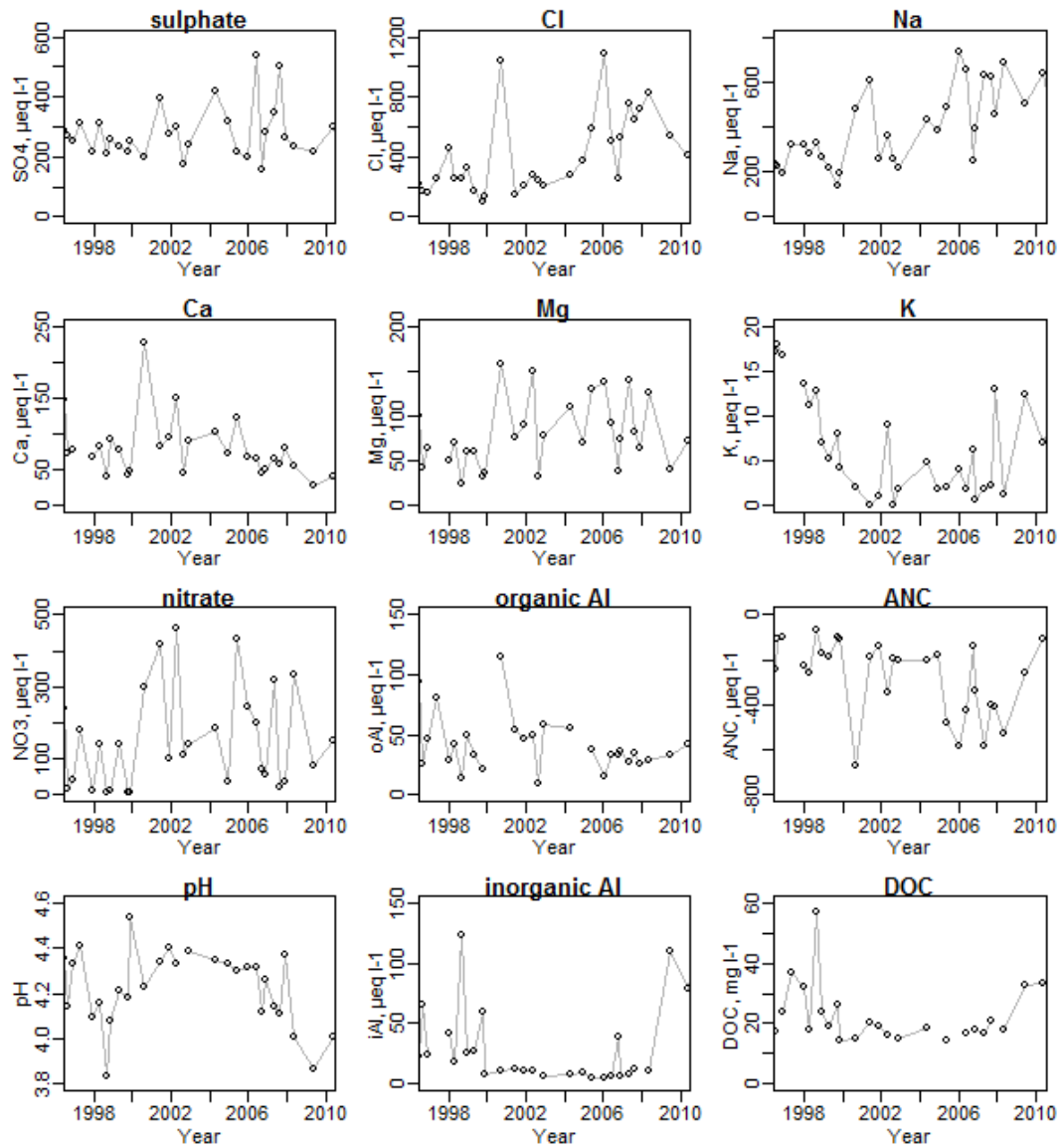
321

Figure 3. Soil solution concentrations of major chemical species monitored (sulphate, Cl⁻, nitrate, DOC, Na⁺, oAl, iAl, Ca²⁺, Mg²⁺, K⁺), ANC and pH at a depth of 50 cm in the Klintaskogen site plot, from 1997–2009.

322

323 **3.2. Model validation and scenarios**

324 *3.2.1. Model validation*

325 Model validation showed good agreement with the monitored data. The model wood biomass before

326 *Lothar*, and the trend of wood biomass change after *Lothar* agreed well with inventory data (Figure 4). For

327 the simulation of soil water chemistry over the period 1997–2009, the measured concentrations of all

328 chemicals were in the range of modeled concentrations, and ForSAFE also captured the temporal

329 dynamics of concentrations for most of chemicals (Figure 5). The model captured two high concentration

330 episodes of N after *Lothar* and after *Gudrun* respectively, and the overall modeled N concentration over

14

331   the period 1997–2009 almost equaled the measured value. The model predicted a decrease in sulphate

332   concentration, but a few measurements outranged the modeled concentration after *Gudrun*. The model

333   simulated two high concentration episodes of BC, one after *Lothar* and one after *Gudrun*, which agreed

334   well with monitored data. But the overall modeled BC concentration was about one-third higher than the

335   measured value. The model reproduced the temporal dynamics of Cl^- concentration, and the overall

336   modeled Cl^- was only 5% more than that of monitored. The modeled Na^+ concentration was generally

337   higher than the monitored over the period 1997–2009.

338
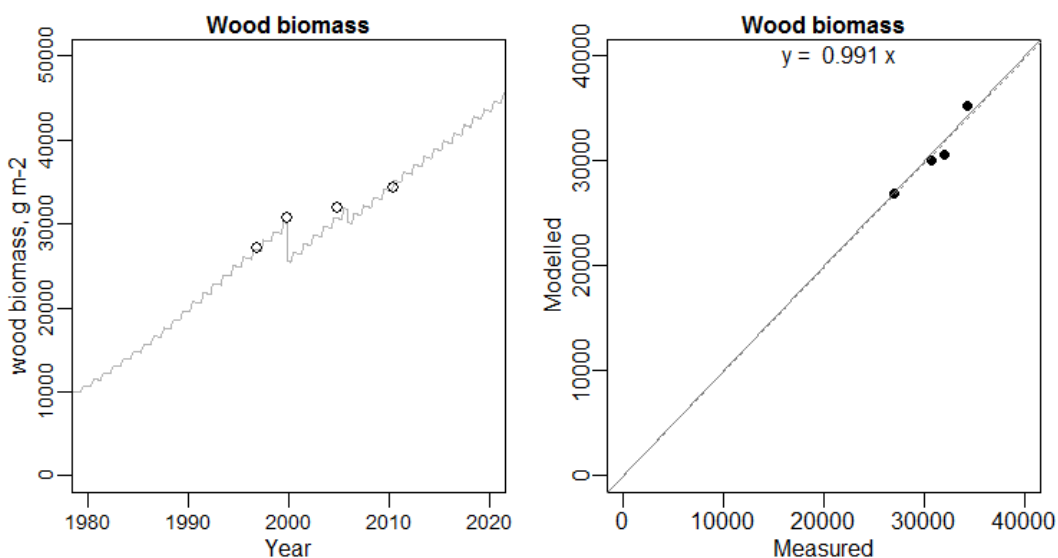
Figure 4. Measured vs. modelled wood biomass. In the left sub-plot, monthly modelled results (grey line) are compared to measured data (points) over the years; in the right sub-plot, the modelled results and measured data are plotted against each other. The dotted line and its slope reported in the equation (y = ax) are an indication of the discrepancy between modelled and measured data.

340

341   However, some discrepancies were observed in the modeling of acidity in soil water. The model

342   overestimated the pH over the period 1997–2009, and the discrepancies were greater before 2000 and after

343   2008 (Figure 5). The prediction of ANC, an important indicator of acidity, well presented the temporal

344   dynamics of measured ANC, but the overall modeled ANC was about 20% higher than the measured value.

345   The DOC concentration, which has a significant effect on pH, was lower in the model than in the

346   measured data. Moreover, the shape of the measured DOC concentration curve was significantly different

347   from the modeled curve.

15
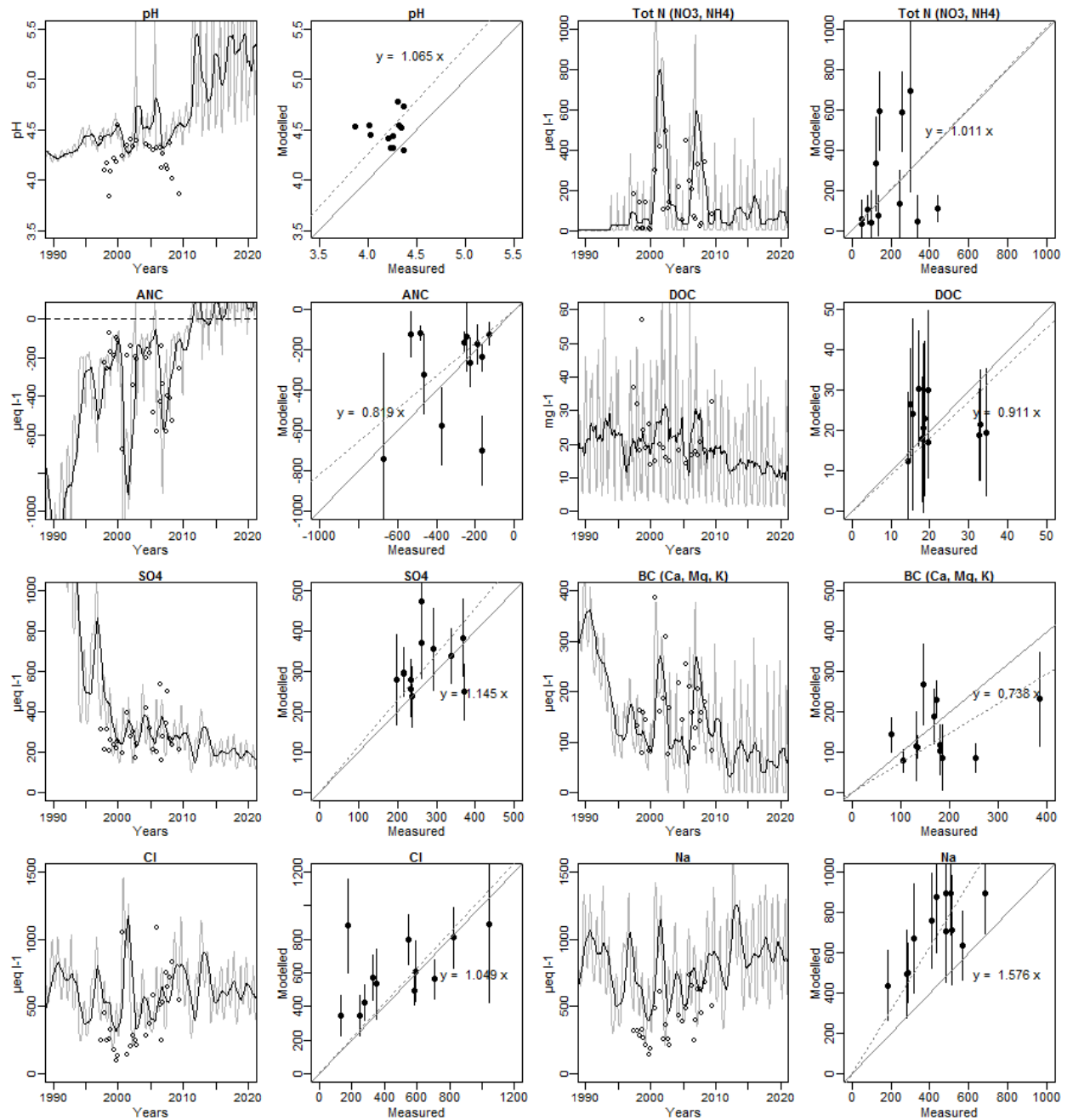
Figure 5. Comparison of modeled and measured soil water chemistry data. The grey curves show the modelled monthly values, and the black lines the moving averages (12-month periods) of these values. ○ – measurements, and ● –yearly mean values. The dotted line and its slope reported in the equation (y = ax) are an indication of the discrepancy between modelled and measured data. The soil water was collected at a depth of 50 cm.

3.2.2. Model scenarios and soil nutrient budget

Clear recovery from the acidification of the 1990s was seen in both the scenarios modelled (Figure 6). This was indicated by a substantial increase in soil solution ANC from –1000 µeq l^{-1} to +100 µeq l^{-1}, and

16

353   by an substantial increase in soil matrix exchangeable base cations from 5 keq ha^{-1} to 35 keq ha^{-1}. A long-

354   term decreasing trend was observed in the modeled BC concentration. The decrease in BC started in the

355   1980s, the concentration decreased from about 1500 µeq l^{-1} to about 100 µeq l^{-1} in the 2000s, by which

356   the modeled BC concentration had reached baseline level.

357   Significant differences were predicted in pH, soil solution N concentration and BC concentration between

358   the BLS scenario and the FSS scenario. Although a long-term increase in pH was predicted in the FSS

359   scenario, strong acidic episodes were seen as the result of storms. Episodes of high concentrations of soil

360   solution N and BC were predicted simultaneously in the FSS scenario in response to storms. Higher soil

361   solution DOC and lower exchangeable BC in soil matrix were also identified in the FSS scenario due to

362   storms. The storm-induced changes in ANC were less profound when comparing the FSS scenario with

363   the BLS scenario.
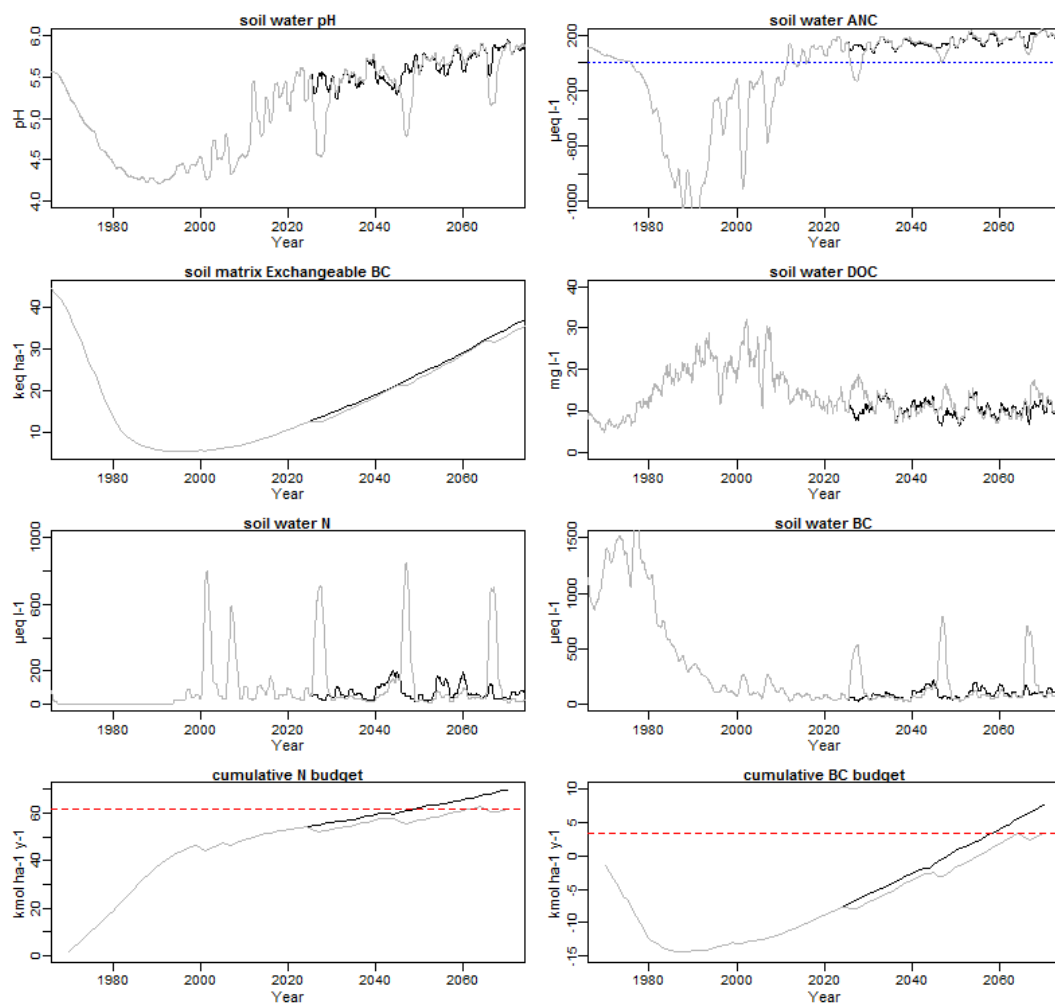
364

Figure 6. Effects of future storm disturbances on soil (BLS: black line; FSS: gray line). Soil water pH, ANC, BC and N concentrations are at 50 cm depth. Exchangeable BC of soil matrix is at layer 5 (Table 2). Cumulative N and BC budget is based on section 2.5, the red dotted lines go through the end of grey lines horizontally.

365

366   N accumulated in the soil in both scenarios over the simulation period 1970–2070 (Figure 6). The rates of

367   accumulation (the slopes of the curve) in most years were positive, but after each storm disturbance, there

368   were a few years with negative values. The rates started to decrease from 1990s and reached a relative

369   stable value after 2010s. Base cations were lost from the soil from 1970, and they started to accumulate

370   from the 1990s, i.e. the rates of accumulation became positive. The rates stabilized after 2010s, and they

371   also shortly became negative after each storm as N did. Differences of cumulative N and BC input-output

372   budget between FSS and BLS could be seen after the first future storm (2025), and they increased after

373   each storm. At 2070, cumulative N and BC budgets were 69.82 and 7.54 kmolc ha^{-1} for BLS, and for FSS

374   they were 61.64 and 3.41 kmolc ha^{-1}. The BLS reached FSS's 2070 level in 2050 and 2058 separately, in

375   other words, the accumulation of N and BC in soil were delayed by storms for about 20 years and 12 years.

4. Discussion

4.1. Recovery from acidification at the Klintaskogen site before Lothar?

378   Klintaskogen is one of the few sites in Sweden which is saturated with both S (Eriksson et al. 1992) and N

379   (Akselsson et al. 2010; Pihl Karlsson et al. 2011) due to high historical acid deposition. We observed a 50%

380   decrease of S deposition from 1997 to 2009, but there was no significant change in N deposition over the

381   period (Figure 2). The change of acid deposition at Klintaskogen over the period 1997–2009 is in line with

382   the findings in many other sites in Sweden (Pihl Karlsson et al. 2011; Akselsson et al. 2013). One

383   consequence of the decreasing sulphate deposition is a reduction in the sulphate concentration in soil water.

384   However, it doesn't necessarily lead to an immediate recovery from the acidification in forest soils (Pihl

385   Karlsson et al. 2011; Akselsson et al. 2013), probably due to the problem of sulphate adsorption

386   reversibility (Reuss & Johnson 1986) and the complexity of acidification and alkalization in soils (Van

387   Breemen et al. 1983). We did not observe significant trends of acidification recovery in soil water before

388   *Lothar* in monitored pH, ANC or iAl (Figure 3).

389   However, the model simulation clearly showed an increase of pH and a decrease of ANC from 1990s

390   (Figure 5 and Figure 6). The main driver for the recovery was the decreased sulphate concentration in the

391   soil water, but another important factor was that no disturbances were simulated between 1990 and 2000.

392   Therefore we can argue that Klintaskogen should recover from acidification from 1990s if no external

393   disturbances happen.

4.2. The influence of Lothar and Gudrun storms on recovery from acidification during 1997–2009

4.2.1. Influence of storms on soil chemistry

396   We observed frequent high-concentration episodes of nitrates, Cl$^-$, Na$^+$ and Mg^{2+} after *Lothar* and *Gudrun*,

397   which could be due to a combination of the sea-salt effect and stimulated mineralization. The temporary

changes in pH, Al^{3+}, Na^+, Cl^- and Mg^{2+} measured at the study site after *Lothar* agree well with the characteristics of the sea-salt effect, which is also supported by the high peak of Cl^- deposition in 1999. The continuous high nitrate concentration could probably be explained by an increase in the mineralization rate due to canopy opening, radiation and temperature change (Vodde et al. 2011).

However, soil water chemistry changed slightly after *Gudrun*. This was a storm with high winds but without heavy precipitation, as could be observed from the monitored throughfall precipitation (data not shown) and total deposition. Therefore, no evidence of sea-salt effect was found in 2005, whereas episodes of remarkably high Cl^-, Na^+ and Mg^{2+} concentrations in 2007 and 2008 indicated two new sea-salt episodes. However, the Ca^{2+} concentration did not increase in the two new sea-salt episodes, and we speculate that this may be due to the greater difficulty for Na^+ to replace Ca^{2+} in more acidified soil (Hindar et al. 1995; Hindar et al. 1994). But the high-nitrate concentration episode had already started in 2005, showing that the increase in mineralization started directly after *Gudrun*.

The sulphate seems to decrease before *Lothar* ($\tau=-0.424$, $p=0.06$). Visual inspection of the data after *Lothar* gives the impression that the amount of sulphate has decreased, but high-concentration episodes occurred more frequently after *Lothar*, disturbing this trend. The reason for the high-concentration episodes could be increased sulphur mineralization from organic matter after storms. This suggests that the long-term decrease in sulphate concentration will be disturbed by future storms.

4.2.2. The influence of storms on soil and water acidity

Higher nitrate leaching was observed after both storms, which are probably due to an increase in organic matter mineralization and an increase in nitrification. It is known that nitrification, in particular when excess production of nitrate (not consumed by plants) occurs, has a very strong acidifying effect (Reuss & Johnson 1986). Meanwhile, nitrate leaching causes base cations leaching.

Although high-concentration episodes of sulphate occurred after *Lothar*, sulphate was not correlated with any cation or ANC, indicating that sulphate is not the main anion regulating ANC or leaching base cations at Klintaskogen.

Sea-salt episodes were observed after *Lothar* and in 2007 and 2008 at Klintaskogen. They are believed to be of little long-term significance since there is often a recovery in soil water after the sea-salt episode temporarily acidifies it (Hindar et al. 1995). It is because that the increased H^+ and Al^{3+} in soil water are actually exchanged from soil matrix, i.e. the total acidity of the whole soil does not increase in a sea-salt episode. Moreover, the recovery from soil acidification may be accelerated due to the additional base cations from the sea-salt episodes (Beier et al. 2003). We observed high correlation between Cl^- and Mg^{2+},

429   indicating that sea-salt episodes also brought a lot of Mg^{2+}. Thus sea-salt episode will probably decrease

430   the soil acidity of Klintaskogen on long term since it replenishes the base saturation.

431   The changes in soil water acidity between 1997 and 2009 reflect the multiple effects of storms, as well as

432   other factors, such as DOC. Before *Lothar*, the variation in pH was driven by the DOC concentration, and

433   indicated by the iAl concentration (Figure 3). The sudden decrease of pH directly after *Lothar* and the

434   subsequent recovery from acidity up till 2002 was explained by the sea-salt effect (Hindar et al. 1995;

435   Evans et al. 2001). Similar temporary acidification and recovery were also identified in 2007 and 2008,

436   when smaller sea-salt episodes were reported also verified by the monitored deposition. The changes in

437   acidity between 2002 and 2007 were generally related to the changes in ANC, with the exception of 2006,

438   when an increment in ANC caused a decrease in pH. This was also characterized by very high Cl^-, Na^+

439   and Mg^{2+} concentrations, indicating a sea-salt episode. However, there was no evidence of a storm in

440   terms of high precipitation or reports by meteorological institutions, and the reason for this exception is

441   still unclear. After 2009, the concentration of DOC increased again, causing another acidification episode.

442   Overall, there was no significant acidification recovery over the period 1997–2009. In contrary, the

443   measured pH decreased significantly due to storms, from 4.54 in Nov. 1999 to 3.86 in May 2009. Given

444   the fact that sea-salt episode has little long-term influence on acidification, the decreased pH is probably

445   driven by nitrification and leaching of nitrate.   Similar decreasing trends of pH were also observed in two

446   other southern Swedish Norway spruce forest sites after 2000, which were both very close to the west

447   coast of Sweden (Akselsson et al. 2013). It indicates that storm disturbances, at sites in close proximity to

448   sea, would cause delay in the acidification recovery. Meanwhile, the considerable effects of DOC

449   concentrations on pH suggest that DOC is also a very important factor and should be included in long-

450   term acidification studies. Visual analysis of the data in this study and the data in Akselsson's study

451   suggests that soil water that contains DOC>20 mg l^{-1} would have much higher pH sensitivity to DOC.

452   **4.3. Long-term effects of frequent storms on future acidification recovery and fertility loss**

453   *4.3.1. Reliability of ForSAFE prediction*

454   **Acidity**: The pH curve obtained with the ForSAFE model exhibited a different shape from the

455   measurements over the monitored period. The model captured the relationship between pH and ANC, but

456   did not predict the strong impact of DOC on pH very well. Neither was the concentration of DOC well

457   predicted. In addition, the pH change caused by sea-salt effect is not readily included in the model yet.

458   Therefore, the difference between the modelled and the measured pH in some cases was larger than half a

459   unit over the period 1997–2009. However, the modeled ANC was well validated by the measured data

460   over the period.

461 In the long term, the effects of sea-salt episodes on acidity is little, and the fact that storms will decrease

462 the ANC in the soil water, regardless the presence of sea-salt episodes, is confirmed by both monitored

463 data and modeled results. Thus the only uncertainty in the long-term modeled pH is DOC. By assuming

464 that no significant change would happen in the DOC concentration on long term in southern Sweden, it is

465 suggested that the modeled long-term trend of acidity change at Klintaskogen is reliable.

466 **Nutrient concentrations:** Both *Lothar* and *Gudrun* caused increases in concentrations of N and BC

467 (Figure 2 and Figure 3), thus increases in leaching and loss of N and BC from the soil (Figure 6). The

468 increased leaching of N after both storms was most probably due to the stimulated mineralization (Legout

469 et al. 2009). The increased leaching of Mg^{2+} after both storms was most probably due to the sea-salt effect,

470 but after *Gudrun*, it was caused by two sea-salt episodes in 2007 and 2008, rather than the storm *Gudrun*.

471 The increased leaching of Ca^{2+} after *Lothar* was due to the sea-salt effect, but after *Gudrun* the leaching of

472 Ca^{2+} decreased to the level before *Lothar*, and we speculate that this may be due to the greater difficulty

473 for Na^+ to replace Ca^{2+} in more acidified soil (Hindar et al. 1995; Hindar et al. 1994). The leaching of K^+

474 was very small, compared with those of Mg^{2+} and Ca^{2+}.

475 ForSAFE well simulated the concentration and temporal dynamics of soil solution N, but some

476 discrepancies were seen in soil solution BC. One important reason is that sea-salt effect was not simulated

477 by the ForSAFE model: Firstly, the base cations are lumped as an equivalent base and are assumed to

478 react as a divalent component BC^{2+} in the soil chemistry module of the model. But sea-salt episodes bring

479 a lot of Mg^{2+} but not Ca^{2+} and the vertical reactive transport of these two elements in the soil profile are

480 very different most especially when the soil contains a high organic matter content (van der Heijden et al.

481 2014).; And secondly, Na^+ is not currently included in the ion-exchange process in the model. Lumped

482 BC^{2+} is satisfactory when studying soil acidification. However finer detail is required to better simulate the

483 nutrient budget, but we believe the model is sufficient for the purposes of this study to obtain an overview

484 of the long-term trend.

485 *4.3.2. Long-term effects of frequent storms on acidification/recovery & fertility*

486 ForSAFE predicts that the Klintaskogen site will slowly recover from acidification in the future. Predicted

487 recovery was slower than prior to 1990s. This recovery is driven by the reduction of S deposition.

488 However, many studies have reported decreasing base cations deposition like Ca^{2+} in north America and

489 Europe over the past decades (Hedin et al. 1994; Watmough et al. 2005; Alewell et al. 2000). This was not

490 simulated here, because no clear evidence of Ca^{2+} deposition reductions was available (Ca^{2+} trend not

491 significant but p=0.06). If Ca^{2+} deposition also decreases in the future, this may further slowdown or invert

492 the recovery trend.

493 The simulation of frequent storms has effects on the soil solution chemistry and N and BC leaching fluxes
494 during the few years after each storm. This caused increased losses of N and BC compared to the BLS
495 scenario (Figure 6). The leaching of nitrate would have strong acidifying effect on soil water and delayed
496 N accumulation in soil, but this would not be an issue for the N fertility of the soil because big amounts of
497 N would accumulated in soils in both scenarios. The leaching of BC would decrease the exchangeable BC
498 of soil, more problematically, lead to severe loss of BC fertility. The future storms (FSS) lead to loss of 12
499 years' accumulation of BC fertility comparing to BLS, which is almost 50% of the total accumulation over
500 the period 1970–2070. However, the recovery indicators (pH, ANC, BC concentration, soil exchangeable
501 BC) in the FSS scenario are not influenced in the long term compared to the BLS scenario, although a
502 temporary acidification episode would be seen after each storm. Furthermore, the comparison between the
503 two scenarios showed that these recovery indicators need about five years or longer to recover from storm
504 disturbances, which was much longer than the observed time to recover from a sea-salt episode. It
505 indicates that the influences of mineralization on acidification recovery are stronger than that of sea-salt
506 episode.

507 Overall, model simulation suggests that storms without sea-salt episodes don't seem to disturb
508 acidification recovery at Klintaskogen on long term. It is in agreement with the finding of Thiffault et al.
509 (2007), that storm disturbances appear not to be the long-term driver of soil chemistry. However, storms
510 raise risks in depleting the BC in the soil. At sites with lower exchangeable pools of Mg^{2+}, Ca^{2+} and K^+,
511 the impact may be more visible.

5. Conclusions

512

513 • The monitoring and the modeled data support the hypothesis that ecosystem disturbances such as
514   storms may strongly influence acidification recovery processes.

515 • There was no monitored evidence proving Klintaskogen was recovering from acidification before
516   2000, but model simulation implied a trend of recovery. The two storms *Lothar* and *Gudrun* strongly
517   disturbed the recovery trend, in fact over the period 1997–2009 some indicators (pH, ANC and Ca^{2+}
518   concentration) suggested that the soil acidification occurred during that period.

519 • Storms occurring with both strong winds (windthrow) and high sea-salt inputs (sea-salt episodes) have
520   an ambiguous effect on acidification recovery. Windthrow and the opening up of the canopy led to
521   increased mineralization/nitrification, thus nitrate and base cations leaching, causing acidification and
522   decreased base saturation; the sea-salt episode led to increased soil water acidity and aluminum
523   concentrations but also possibly replenished the soil cation exchange pool with Mg^{2+}, thus on long
524   term increasing the soil pH buffer capacity.

525 • No evidence that frequently (20 years) occurring storms with windthrow hamper acidification
526   recovery but storms may influence soil fertility by losses of base cations. This may be a concern for
527   the most base cation poor forest soils.

Acknowledgment

References

Akselsson, C. et al., 2013. Acidification trends in south Swedish forest soils 1986-2008 — slow recovery and high sensitivity to sea-salt episodes. *The Science of the total environment*, 444, pp.271–287.

Akselsson, C. et al., 2010. Assessing the risk of N leaching from forest soils across a steep N deposition gradient in Sweden. *Environmental pollution*, 158(12), pp.3588–3595.

Akselsson, C. et al., 2007. Nutrient and carbon budgets in forest soils as decision support in sustainable forest management. *Forest Ecology and Management*, 238(1-3), pp.167–174.

Alewell, C. et al., 2000. Effects of reduced atmospheric deposition on soil solution chemistry and elemental contents of spruce needles in NE—Bavaria, Germany. *Journal of Plant Nutrition and Soil Science*, 163(5), pp.509–516.

Attiwill, P.M. & Adams, M.A., 1993. Nutrient cycling in forests. *New Phytologist*, 124(50), pp.561–582.

Balland, V., Pollacco, J. a. P. & Arp, P. a., 2008. Modeling soil hydraulic properties for a wide range of soil conditions. *Ecological Modelling*, 219(3-4), pp.300–316.

Beier, C., Moldan, F. & Wright, R.F., 2003. Terrestrial ecosystem recovery—modelling the effects of reduced acidic inputs and increased inputs of sea-salts induced by global change. *Ambio*, 32(4), pp.275–282.

Belyazid, S., Westling, O. & Sverdrup, H., 2006. Modelling changes in forest soil chemistry at 16 Swedish coniferous forest sites following deposition reduction. *Environmental pollution*, 144(2), pp.596–609.

Brandtberg, P.-O. & Olsson, B. a., 2012. Changes in the effects of whole-tree harvesting on soil chemistry during 10 years of stand development. *Forest Ecology and Management*, 277, pp.150–162.

Van Breemen, N., Mulder, J. & Driscoll, C.T., 1983. Acidification and alkalinization of soils. *Plant and Soil*, 75(3), pp.283–308.

Dahlgren, R.A. & Driscoll, C.T., 1994. The effects of whole-tree clear-cutting on soil processes at the Hubbard Brook Experimental Forest, New Hampshire, USA. *Plant and Soil*, 158(2), pp.239–262.

DeLuca, T. et al., 2002. Quantifying nitrogen-fixation in feather moss carpets of boreal forests. *Nature*, 419(October), pp.917–920.

Eriksson, E., Karltun, E. & Lundmark, J., 1992. Acidification of in Sweden Forest. *Ambio*, 21(2), pp.150–154.

566 Evans, C.D., Monteith, D.T. & Harriman, R., 2001. Long-term variability in the deposition of
567   marine ions at west coast sites in the UK Acid Waters Monitoring Network: impacts on
568   surface water chemistry and significance for trend determination. *The Science of the Total*
569   *Environment*, 265(1-3), pp.115–129.

570 Gundersen, P., Schmidt, I.K. & Raulund-Rasmussen, K., 2006. Leaching of nitrate from
571   temperate forests — effects of air pollution and forest management. *Environmental Reviews*,
572   14, pp.1–57.

573 Hedin, L.O. et al., 1994. Steep declines in atmospheric base cations in regions of Europe and
574   North America. *Nature*, 367, pp.351–354.

575 Van der Heijden, G. et al., 2013. Assessing Mg and Ca depletion from broadleaf forest soils and
576   potential causes – A case study in the Morvan Mountains. *Forest Ecology and Management*,
577   293, pp.65–78.

578 Van der Heijden, G. et al., 2014. The dynamics of calcium and magnesium inputs by throughfall
579   in a forest ecosystem on base poor soil are very slow and conservative: evidence from an
580   isotopic tracing experiment (26Mg and 44Ca). *Biogeochemistry*, 118(1-3), pp.413–442.

581 Hindar, A. et al., 1994. Acid water and fish death. *Nature*, 372, pp.327–328.

582 Hindar, A. et al., 1995. Extreme acidification in small catchments in southwestern Norway
583   associated with a sea salt episode. *Water, Air, & Soil Pollution*, 85, pp.547–552.

584 HruŠka, J. et al., 2012. Long-term forest soil acidification, nutrient leaching and vegetation
585   development: Linking modelling and surveys of a primeval spruce forest in the Ukrainian
586   Transcarpathian Mts. *Ecological Modelling*, 244, pp.28–37.

587 Iwald, J. et al., 2013. Acidifying effect of removal of tree stumps and logging residues as
588   compared to atmospheric deposition. *Forest Ecology and Management*, 290, pp.49–58.

589 Johns, T.C. et al., 2006. The New Hadley Centre Climate Model (HadGEM1): Evaluation of
590   Coupled Simulations. *Journal of Climate*, 19, pp.1327–1353.

591 Jonard, M. et al., 2015. Tree mineral nutrition is deteriorating in Europe. *Global Change Biology*,
592   21, pp.418–430.

593 Laudon, H., 2008. Recovery from episodic acidification delayed by drought and high sea salt
594   deposition. *Hydrology and Earth System Sciences*, 12(2), pp.363–370.

595 Legout, A. et al., 2009. Effects of storm Lothar (1999) on the chemical composition of soil
596   solutions and on herbaceous cover, humus and soils (Fougères, France). *Forest Ecology and*
597   *Management*, 257(3), pp.800–811.

598 Lundell, Y., Johannisson, C. & Ho, P., 2001. Ion leakage after liming or acidifying fertilization of
599   Swedish forests — a study of lysimeters with and without active tree roots. *Forest Ecology*
600   *and Management*, 147, pp.151–170.

601 Marklund, L.G., 1988. *Biomass functions for pine, spruce and birch in Sweden*.

602 McLeod, A.I., 2011. *Kendall: Kendall rank correlation and Mann-Kendall trend test.* R package
603   version 2.2.

604 Milsom, J., 2003. *Field Geophysics* 3rd ed., West Sussex: Wiley.

605 Nakicenovic, N. et al., 2000. *IPCC Special Report: Summary for Policymakers Emissions*
606   *Scenarios*, Geneva.

607 Navrátil, T. et al., 2007. Acidification and recovery of soil at a heavily impacted forest catchment
608   (Lysina, Czech Republic)-SAFE modeling and field results. *Ecological Modelling*, 205(3-4),
609   pp.464–474.

610 Oulehle, F., Hofmeister, J. & Hruška, J., 2007. Modeling of the long-term effect of tree species
611   (Norway spruce and European beech) on soil acidification in the Ore Mountains. *Ecological*
612   *Modelling*, 204(3-4), pp.359–371.

613 Pedersen, L.B. & Bille-Hansen, J., 1995. Effects of airborne sea salts on soil water acidification
614   and leaching of aluminium in different forest ecosystems in Denmark. *Plant and Soil*, 168-
615   169(1), pp.365–372.

616 Pihl Karlsson, G. et al., 2011. Reduced European emissions of S and N—effects on air
617   concentrations, deposition and soil water chemistry in Swedish forests. *Environmental*
618   *pollution*, 159(12), pp.3571–82.

619 Posch, M. & Kurz, D., 2007. A2M—A program to compute all possible mineral modes from
620   geochemical analyses. *Computers & Geosciences*, 33(4), pp.563–572.

621 R Core Team, 2013. *R: A Language and Environment for Statistical Computing.* Vienna, Austria.

622 Ranger, J. & Turpault, M.-P., 1999. Input–output nutrient budgets as a diagnostic tool for
623   sustainable forest management. *Forest Ecology and Management*, 122(1-2), pp.139–154.

624 Reuss, J.O. & Johnson, D.W., 1986. *Acid deposition and the Acidification of Soils and Waters*,
625   New York: Springer-Verlag.

626 Schlyter, P. et al., 2006. Assessment of the impacts of climate change and weather extremes on
627   boreal forests in northern Europe , focusing on Norway spruce. *climate research*, 31, pp.75–
628   84.

629   Simpson, D. et al., 2011. Atmospheric transport and deposition of reactive nitrrogen in Europe. In
630   M. A. Sutton et al., eds. *The European Nitrogen Assessment*. Cambridge: Cambridge
631   University Press, pp. 298–316.

632   Staelens, J. et al., 2008. Calculating Dry Deposition and Canopy Exchange with the Canopy
633   Budget Model: Review of Assumptions and Application to Two Deciduous Forests. *Water,*
634   *Air, and Soil Pollution*, 191(1-4), pp.149–169.

635   Sverdrup, H. et al., 2006. Assesing nutrient sustainability of forest production for different tree
636   species considering Ca, Mg, K, N and P at Björnstorp Estate, Sweden. *Biogeochemistry*,
637   81(2), pp.219–238.

638   Sverdrup, H. et al., 2005. Modeling recovery of Swedish ecosystems from acidification. *Ambio*,
639   34(1), pp.25–31.

640   Sverdrup, H. & Rosen, K., 1998. Long-term base cation mass balances for Swedish forests and
641   the concept of sustainability. *Forest Ecology and Management*, 110(1-3), pp.221–236.

642   Sverdrup, H. & Warfvinge, P., 1993. Calculating field weathering rates using a mechanistic
643   geochemical model PROFILE. *Applied Geochemistry*, 8(3), pp.273–283.

644   Tamm, C.O., 1991. *Nitrogen in Terrestrial Ecosystems* W. D. Billings et al., eds., Berlin:
645   Springer-Verlag.

646   Thiffault, E. et al., 2007. Investigating the soil acid-base status in managed boreal forests using
647   the SAFE model. *Ecological Modelling*, 206(3-4), pp.301–321.

648   Vodde, F. et al., 2011. The influence of storm-induced microsites to tree regeneration patterns in
649   boreal and hemiboreal forest. *Journal of Forest Research*, 16(3), pp.155–167.

650   Vygodskaya, N.N. et al., 2002. Climatic control of stand thinning in unmanaged spruce forests of
651   the southern taiga in European Russia. *Tellus*, 54B(5), pp.443–461.

652   Wallman, P. et al., 2005. ForSAFE—an integrated process-oriented forest model for long-term
653   sustainability assessments. *Forest Ecology and Management*, 207(1-2), pp.19–36.

654   Warfvinge, P. & Sverdrup, H., 1995. Critical loads of acidity to Swedish forest soils. In *Reports*
655   *in Environmental Engineering and Ecology*. Lund, Sweden: Lund University.

656   Wastenson, L. et al. eds., 1990. *National Atlas of Sweden: The Forest* 1st ed., Enköping: SNA.

657   Watmough, S. a et al., 2005. Sulphate, nitrogen and base cation budgets at 21 forested catchments
658   in Canada, the United States and Europe. *Environmental monitoring and assessment*, 109(1-
659   3), pp.1–36.

660 Wright, R.F. et al., 1988. Experimental verification of episodic acidification of freshwaters by sea
661   salts. *Nature*, 334, pp.422–424.

662 Wright, R.F., 2008. The decreasing importance of acidification episodes with recovery from
663   acidification: an analysis of the 30-year record from Birkenes, Norway. *Hydrology and*
664   *Earth System Sciences*, 12(2), pp.353–362.

665 Zanchi, G. et al., 2014. Modelling the effects of management intensification on multiple forest
666   services: a Swedish case study. *Ecological Modelling*, 284, pp.48–59.

667